Contributions of winter and spring warming to the temporal shifts of leaf unfolding

Haicheng Zhang (haicheng.zhang@ulb.ac.be)
Department Geoscience, Environment & Society, Université Libre de Bruxelles

Pierre Regnier
Université Libre de Bruxelles

Isabelle Chuine
CNRS https://orcid.org/0000-0003-3308-8785

Philippe Ciais
Laboratoire des Sciences du Climat et de l'Environnement https://orcid.org/0000-0001-8560-4943

Wenping Yuan
Sun Yat-sen University https://orcid.org/0000-0002-1469-4395

Article

Keywords: temporal shifts, climate change, spring phenology, winter and spring temperatures

Posted Date: June 17th, 2021

DOI: https://doi.org/10.21203/rs.3.rs-505838/v1

Target journal: *Nature Climate Change*

Contributions of winter and spring warming to the temporal shifts of leaf unfolding

Haicheng Zhang[1], Pierre Regnier[1], Isabelle Chuine[2], Philippe Ciais[3], Wenping Yuan[4]

[1]Department Geoscience, Environment & Society-BGEOSYS, Université libre de Bruxelles, 1050 Bruxelles, Belgium.

[2] CEFE, Univ Montpellier, CNRS, Univ Paul Valéry Montpellier 3, EPHE, IRD, Montpellier, FR-34293, cedex 5, France.

[3]Laboratoire des Sciences du Climat et de l'Environnement, IPSL-LSCECEA/CNRS/UVSQ Saclay, 91191, Gif-sur-Yvette, France.

[4]School of Atmospheric Sciences, Sun Yat-sen University, Zhuhai, Guangdong 510245, China.

Corresponding author: Haicheng Zhang (*haicheng.zhang@ulb.be*)

Abstract (150 words) Changes in winter and spring temperatures have been widely used to explain the diverse responses of spring phenology to climate change. However, our understanding of their respective roles remain incomplete. Using >300,000 *in situ* observations of leaf unfolding date (LUD) in Europe, we show that the advancement of LUD since 1950 is due both to accelerated spring thermal accumulation and changes in winter chilling which explain 61% and 39% of the LUD shifts, respectively. Winter warming did not substantially retard the releasing of bud dormancy, but increased the thermal requirement to reach leaf unfolding. The increase of thermal requirement and decreased efficiency of spring warming on accelerating thermal accumulation partly explained the temporally (1950s-2010s) decreasing response of LUD to warming. Our study stresses the need to better assess the antagonistic and heterogeneous effects of winter and spring warming on leaf phenology, which is key to projection of future vegetation-climate feedbacks.

Timing of leaf unfolding influences the duration of plant growing season, and therefore their productivity, as well as land-surface physical properties like the surface albedo and roughness[1-3]. Shifts in leaf unfolding date (LUD) may also alter competition between plants, community structure and ecosystem water, carbon and nutrient cycles[4-6]. Many studies based on both *in situ* observations and satellite-derived data have reported a general trend of advancing spring leaf phenology during the past decades, in particular LUD, in response to climate warming in temperate and boreal regions[7-11]. However, although there is now mounting evidence that the spring leaf phenology as a whole is shifting earlier in time, the magnitude (or even direction) of this shift shows significant taxonomic, temporal and spatial variations[12-16]. In particular, the sensitivity of LUD to climate warming (S_T, day °C^{-1}), defined as the shift in LUD per °C warming, has significantly declined over the past 30 years in many regions[7,17].

Temperature has been regarded as the most important environmental factor controlling plant phenology[18]. Plants in temperate and boreal regions generally require a certain number of days with cold temperatures to release bud dormancy, and subsequently, a certain number of days with warmer conditions (called forcing temperatures) to trigger cell growth and leaf development[19-22]. Several studies have argued that changes in winter chilling and thermal accumulation caused by climate change explain the divergent responses of LUD to rising temperature[7,23-26]. Especially, winter warming can affect LUD through two distinct effects: it may delay the timing of bud dormancy release, and may increase the thermal requirement for bud break[27,28]. Indeed, experimental studies have shown that the thermal requirement for bud break depends on the amount of winter chilling, that is, the more chilling received, the lower the thermal requirement to reach bud break[20,29]. These two opposing effects might

explain why the sensitivity of LUD to warming has significantly declined over the past 30 years of warming[7,24]. They might also explain why some species have shown scant or no advances in LUD with climate warming[8,23,25]. Even so, the impacts of climate warming on winter chilling, spring thermal accumulation and the resulting shifts in LUD have not been quantitatively estimated for multiple species at large spatial scale, in particular when considering the asynchronicity of winter and spring warming[24,30,31]. Moreover, our mechanistic understanding of the shifts in LUD in response to warming is still far from complete[32], especially regarding the observed decline in the sensitivity of LUD to continuously rising temperature[7]. This incomplete understanding limits our ability to project regional and global changes in LUD under future climate warming, as well as the resulting changes in ecosystem structure and functions.

Here, we take a new step forward to advance our quantitative and mechanistic understanding in ongoing changes in leaf phenology. Using long-term (1951-2019) *in situ* observation data of LUD for six dominant tree species collected at 2945 sites in central Europe[33] (see Methods and Fig. S1 in Supplementary Information, SI), this study aims to 1) quantify the relative contribution of changes in winter and spring warming to the temporal shifts in LUD in Europe; 2) elucidate the mechanisms that can explain explain the declining sensitivity of LUD to rising temperature, as observed over the past three decades[7].

To achieve these aims, we applied the Unified phenology model[19,28] at each of the 2945 observation sites for each tree species (see Methods). Plant phenological models describe the causal relationships between winter and spring temperatures and bud development[34,35]. Existing phenological models (e.g. the Thermal Time, Sequential, Parallel and Alternating models) generally rely on distinct assumptions regarding the

response of bud growth to spring thermal accumulation and/or winter chilling[34,35](see Methods). The advantage of the Unified model used here is that it integrates these different assumptions, and each of the earlier models can be regarded as particular cases of the Unified model (see Methods and Fig. S2). A previous study also reported that the Unified model provides a more accurate estimation of LUD in Europe than other commonly used models[7]. For these reasons, we used the Unified model to disentangle the various effects of climate warming on LUD.

Contributions of winter and spring warming to the temporal shifts in LUD

According to the Unified model[19] (see Methods for details), bud dormancy is assumed to be released when chilling accumulation meets plants' critical requirements (CHA_0 in Fig. S2). The forcing stage starts as soon as this chilling requirement is met and leaf unfolding occurs when the thermal accumulation during the forcing stage exceeds a given threshold. This threshold, denoted by TA_0, declines exponentially with the total amount of chilling received during the whole pre-growing season (CHA_{tot}, Fig. S2b), defined as the period from the onset of chilling accumulation till the LUD. Therefore, the temporal shifts in LUD are determined by the time when bud dormancy is released (d_{f0}), which in turn depends on the chilling accumulation rate (CH_r, Eq. 1), by the thermal accumulation rate (F_r, Eq. 2), and by the required amount of thermal accumulation (TA_0, Eq. 3) which in turn depends on the total amount of chilling (CHA_{tot}, Eq. 4) received before the LUD (Fig. S2).

The Unified model with nine optimized model parameters (see Methods and Table S2) captured well the observed LUD for each species at each site (Fig. S3). For the six species considered here (*Aesculus hippocastanum*, *Alnus glutinosa*, *Betula pendula*, *Fagus sylvatica*, *Fraxinus excelsior* and *Quercus robur*, Table S1), the model

105 explained 60-80% of the spatiotemporal variations in LUDs (Fig. S3). For
106 approximately 90% of the entire phenological records (1951-2019), the absolute error
107 in simulated LUDs were shorter than one week (Fig. S3) which is the observation
108 interval of the phenological data used in this study[33].

109 The average LUDs advanced by 1.9 (±2.3, standard deviation of both inter-site and
110 inter-species variations) and 5.8 (±2.9) days during the periods 1980-1999 and 2000-
111 2019, respectively, compared to the reference period 1951-1979 (ΔLUD, Fig. 1a and
112 Fig. S4). Changes in LUD over time for the different species were overall similar, the
113 inter-species differences in average LUD advancement rarely exceed one day for both
114 two periods. Yet, differences in LUD temporal shifts were larger across sites whatever
115 the species, ranging from an advance of more than 10 days to a delay of more than 2
116 days (Figs. S4 & S6). Generally, advances in LUD occurred more often at sites with
117 stronger warming (e.g. northern Germany), while delays in LUD mostly occurred at
118 sites with temperature declines (e.g. southeastern Germany and Austria) during the
119 period 1951-2019 (Figs. S6 & S7). 1 °C rise in mean annual temperature, mean spring
120 temperature and mean winter temperature resulted in an average advance in LUD by
121 4.4 (±1.8), 3.2 (±1.2) and 1.4 (±0.7) days in central Europe, respectively (Fig. S8).

122 Advances in LUD were mainly caused by the acceleration in thermal accumulation
123 induced by the warming of spring (ΔD_{FD}, Fig. 1). For the periods 1980-1999 and
124 2000-2019, the durations of the forcing stage were 4.0 (±3.8) and 8.7 (±7.0) days
125 shorter than during the period 1951-1979, respectively. In contrast, the increase in
126 thermal requirements (TA_0) induced by the decline in total preseason chilling
127 accumulation (CHA_{tot}) delayed LUDs by 1.2 (±1.6) and 2.3 (±2.0) days in 1981-2000
128 and 2000-2019 respectively, compared to the earlier period (ΔD_{TA0}, Fig. 1). Changes
129 in dormancy release day (ΔD_{df0}, which is also the onset of the forcing stage)

130 contributed less to the shifts in LUDs, generally by less than 2 days. From the period
131 1951-1979 to the periods 1980-1999 and 2000-2019, the dormancy release day
132 advanced by 0.3 (±2.1) and 1.7 (±3.9) days on average, respectively (Fig. 1a).
133 Temporal shifts in dormancy release day differed significantly across species and
134 were overall larger for *Fraxinus excelsior* and *Quercus robur*, which have
135 comparatively later LUDs (Fig. S9) than other species (Figs. 1 and S4). Overall, the
136 changes in duration of forcing accumulation (ΔD_{FD}), plants' thermal requirement
137 (ΔD_{TA0}) and dormancy release day (ΔD_{df0}) between the reference period 1951-1979
138 and the most recent period 2000-2019 explained 61%, 22% and 17% of the total LUD
139 advance (Fig. 1b). In other words, the acceleration in thermal accumulation caused by
140 climate warming (ΔD_{FD}) explained 61% of the temporal shift in LUD, while changes
141 in chilling accumulation ($\Delta D_{df0}+\Delta D_{TA0}$) explained the remaining 39% through their
142 influence on plants' thermal requirement and dormancy release day (Fig. 1b).

143 **Revealing the complex and antagonistic effects of temperature on LUD**

144 The warming-induced change in the dormancy release day has been widely invoked to
145 explain why the LUDs of some plants show a weak or no delayed shifts with climate
146 warming[7,8,16]. A common hypothesis relies on the premises that warm temperatures in
147 winter delay the timing at which chilling requirements for dormancy release are met,
148 therefore postponing the start of the forcing stage and mitigating the advancement of
149 the LUD caused by the spring warming. Our results however suggest that the winter
150 warming only marginally changed the timing of dormancy release, especially from
151 1951-1979 to 1980-1999 (Fig. 1). At more than 98% of the sites, the optimized
152 functions for calculating daily chilling rates showed an optimum (see the pattern
153 plotted in Fig. S10b), with the optimal chilling temperature (T_{op}) mostly varying
154 between 0 °C and 12 °C with a mean value of 6.5 (±2.1) °C (Fig. S11c). Therefore,

155 the widely used index-chilling days[20,35] (Fig. S10a), which assumes identical effect of
156 chilling temperature below a threshold, was less efficient in explaining the observed
157 LUD and, thus, was not retained by the optimization algorithm. Winter temperatures
158 recorded at the observation sites were mostly 3 to 12 °C lower than the local T_{op}
159 during the period 1951-1979, and then gradually increased towards T_{op} with time (Fig.
160 2a). This decreasing difference between winter and optimal chilling temperatures
161 translated into an important increase in the chilling rates during winter days when
162 temperatures are lower than T_{op} (e.g. days between d_{c1} and d_{c2} in Fig. 3). As a result
163 of these increased chilling rates, the warming-induced loss in chilling rates in late
164 autumn and early spring (e.g. days before d_{c1} and days after d_{c2} in Fig. 3) were
165 actually partly or sometimes even fully offset. This explains why the dormancy
166 release days (ΔD_{df0}) for all species were not substantially postponed and were in fact
167 mostly occurring slightly earlier in time (Figs. 1 and S4).

168 The decrease in chilling accumulation rates after dormancy release from the period
169 1951-1979 to 2000-2019 because of the moving away of temperature from T_{op} due to
170 the warming of spring (Figs. 2b and 3), additionally resulted in an overall decrease of
171 the total amount of chilling accumulated before bud break (Fig. 2c). As a result,
172 while dormancy could be released earlier due to more efficient chilling in cool winter
173 during the last decades, the total chilling accumulation declined by 0.8(±0.9)% on
174 average from 1951-1979 to 1980-1999, and by 2.0(±1.2)% from 1951-1979 to 2000-
175 2019 (Fig. 2c). This decline translated into a slight but significant increase in the
176 critical forcing accumulation required for leaf unfolding (TA0), by 0.5(±0.5)% and
177 1.2(±0.8)% between the reference period and the periods 1981-2010 and 2000-2019,
178 respectively (Fig. 2d). This slight increase in TA0 was however largely compensated
179 by an important increase of the forcing rate (F_r, Fig. 2e) during spring of 8.9(±10.4)%

and 22.9(±13.9)% between the reference period and the 1981-2010 and 2000-2019 periods respectively. As a result, the plants' thermal requirements were reached within a shorter time interval in the recent decades compared to the period 1951-1979, resulting in a significant advancement of the LUD (Fig. 1).

Why does the temperature sensitivity of LUD decline with climate warming?

Consistent with previous studies conducted in Europe and China[7,17], we also find a general decline in temperature sensitivity of LUD (S_T, i.e. change in LUD per °C warming), although this decline seems to have stopped in the last 20 years in central Europe (Fig. S12). Linear regression between S_T and different metrics of winter chilling and forcing temperature reveal that the average daily chilling rate during the dormancy stage (CH_{rave} from d_{c0} to d_{f0}), the total chilling accumulation during the whole pre-growing season (CHA_{tot} from d_{c0} to LUD) and the average daily forcing rate during the forcing stage (F_{rave} from d_{f0} to LUD) across all sites explained 17.6(±18.3)%, 18.4(±18.9)% and 21.0(±20.5)% of the temporal variation of S_T on average, respectively (Fig. 4). CH_{rave} and CHA_{tot}, which together represents the overall impacts of winter chilling on LUD, explained 33.4(21.5)% of the variation in S_T. By further including F_{rave}, the three metrics together accounted for 44.5(±21.0)% of the variation in S_T. The forcing duration (FD) alone, which is determined by CHA_{tot} and F_{rave}, explained 21.3(20.6)% of the variation in S_T. Irrespective of the metrics, their explanatory power varied drastically among observation sites, as demonstrated by the large interquartile (thick) and 95% confidence intervals of the R^2 in Fig. 4. Note that the pre-growing season for calculating S_T in Fig. 4 is defined as the period from d_{c0} to LUD and thus differs from the one applied in several previous studies[7,17,36]. In earlier work, the pre-growing season was usually defined as the period for which the absolute value of the correlation coefficient between LUD and air

205 temperature was largest (i.e. the period which is most relevant to leaf unfolding, see
206 Methods). Nevertheless, our analysis suggests that the abilities of different chilling
207 and forcing metrics to explain the S_T variation calculated based on these two distinct
208 definitions of the pre-growing season were overall similar (Figs. 4 and Fig. S13).

209 Changes in winter chilling due to warming have been proposed as the main
210 explanation of the temporal variation in S_T[7,17]. Our results show that the overall effect
211 of winter warming on S_T is indeed higher than that of spring warming. They further
212 support the hypothesis that winter warming results in a decline of S_T by inducing a
213 decrease in the total amount of chilling received and a subsequent increase in the
214 critical forcing requirements for leaf unfolding (Figs. 2, 4 and Eq. 3). However, they
215 do not support the hypothesis that winter warming leads to a decline of S_T by delaying
216 the timing of dormancy release (d_{f0}), at least up to 2019. Indeed, while changes in
217 CH_{rave} due to winter warming can induce changes in d_{f0} (Fig. 2) and explain a part of
218 the temporal variation in S_T (Fig. 4), we found very limited changes in CH_{rave} and d_{f0}.
219 In fact, at many observation sites, d_{f0} actually occurred slightly earlier and not later in
220 time in response to the winter warming (Figs. 1 and S4).

221 For all species, the increase of forcing rate consistently explained more variation in S_T
222 than did chilling rate and chilling accumulation taken alone (Fig. 4). Since dormancy
223 break date did not change significantly (Fig. 1) and the forcing rate increased
224 substantially, the duration of the forcing stage decreased which explained most of the
225 advancement in LUD. Therefore, the variation in S_T was, to date, also strongly
226 dependent on the duration of the forcing stage and the average temperature during this
227 stage. For example, in Fig. 3, when the LUD advances from d_0 to d_{0+6}, the forcing
228 temperatures on days between d_{0+6} and d_0 become useless to leaf unfolding (but still
229 useful to late leaf growing). The daily average forcing rate (F_{rave}) from d_{f0} to d_{0+3} in

the year with +3 °C warming (Y_{0+3}) has to be larger than the F_{rave} from d_{f0} to d_0 in the reference year Y_0, and the increment of F_{rave} from Y_{0+3} to the year with +6 °C warming (Y_{0+6}) should be even larger than the increment from year Y_0 to Y_{0+3}, due to the further decreased DF. This explains why the temperature sensitivity of LUD is significantly related to the DF (Fig. 4).

The weakening effect of spring warming on S_T can be explained by the non-linear shape of the relationship between daily forcing rate (F_r) and daily mean temperature (Eq. 2). At most sites, this relationships indeed followed a sigmoid pattern (e.g. forcing rate presented in Fig. S2a), rather than a nearly linear change pattern as the widely used forcing metric-growing degree-days (defined as the difference between daily mean temperature and a base temperature, e.g. Fig. S10d). Therefore, the effects of warming on accelerating forcing accumulation increases as temperature moves towards T_{50}, the temperature inducing 50% of optimal growth in forcing rate and the inflection point of the function, but decreases as temperature moves away from T_{50}. For example, in Fig. S2a, the forcing rate increases substantially when daily temperature rises from 5 °C to 10 °C, but increases limitedly when the temperature further rises to 15 °C. The T_{50} estimates in Europe mostly varied between 8 to 11°C on average (Fig. S11). In 1951-1979, the temperature during the forcing stage was 0.35(±2.36) °C lower than T_{50} on average (Fig. S14). However, in 1980-1999 and 2000-2019, the temperatures during the forcing stage were 0.08(±2.28) and 1.55(±2.51) °C higher than T_{50} on average, respectively. Therefore, spring mean temperature moved towards T_{50} from 1951-1979 to 1980-1999 while it moved away from it afterwards, which explains why the effect of warming on accelerating forcing accumulation decreased the last 20 years while it had increased in the earlier periods.

Although temperature is the dominant factor of spring phenology[18], other factors, especially photoperiod, may also influence the response of LUD to climate warming in some species[5,37]. Temperature can vary strongly within a short time (e.g. a few days) and may show large interannual variations. Sensitivity to photoperiod protects plants from the potentially fatal consequences (e.g. frost damage) short warm spells during autumn and winter[38]. Photoperiod has also been shown to impact bud growth after dormancy break for a few species, among which *Fagus sylvatica* which shows the greatest sensitivity to this factor[39,40]. Our results indeed reveal that the three temperature metrics (CH_{rave}, CH_{tot} and F_{rave}) together explain less than half of the temporal changes in S_T at many sites (Fig. 4). Therefore, part of the remaining variation might be explained by an effect of photoperiod. In addition, we found that the relationships between temperature sensitivity of LUD and the duration of the forcing stage and the forcing rate are likely nonlinear at many sites (e.g. Fig. S15). Using linear regression functions may therefore underestimate the impacts of these variables on the temporal variation of S_T.

Understanding the controlling mechanism of climate warming on LUD is important for accurately projecting future vegetation dynamics and ecosystem carbon cycle[5,37]. This study quantified the potential contributions of warming-induced changes in dormancy release day, forcing rate and thermal requirement for leaf unfolding to the advances of LUD of six dormant tree species in central Europe. It showed that the overall effect of the winter warming explained most of the decline in the sensitivity of LUD to temperature in Europe from 1951-2019 although not through a delayed dormancy break date. It showed additionally that the spring warming by increasing the forcing rate and thereby decreasing the duration of the forcing stage also explained a large part of the decline in the temperature sensitivity of LUD because of

a lower increase of forcing rate per degree warming. Our results revealed the importance of representing the antagonistic effects and their inhomogeneous effectiveness of the chilling and forcing temperatures on bud development, especially when considering the seasonally asynchronous climate change[30,31]. These results are helpful to improve the simulation of plant phenology in earth system models, therefore decreasing the uncertainties in projections of future vegetation dynamics and carbon cycle-climate feedbaks. Note that our findings are based on phenological observations from central Europe, they may not hold true for other regions. Therefore, we encourage more studies based on global field observations or control laboratory experiments to further explore the mechanisms driving plant phenology in a larger range of climatic conditions.

Methods

Phenological and climatic data Phenological dataset of leaf unfolding day (LUD) during the period 1951- 2019, as well as the geographical location and elevation for each observation site, were obtained from the Pan European Phenology (PEP) network (http://www.pep725.eu), an open access repository of *in situ* phenological records for multiple plant species across Europe[33]. The LUDs were defined by the BBCH (Biologische Bundesanstalt, Bundessortenamt und Chemische Industrie) code as stage 11 (first leaf unfold). Specifically, we selected the LUD records of the six mostly observed tree species at 2,944 sites in central Europe (Table S1 and Fig. S1 in Supplementary Information (SI)). For each species, only the sites with phenological observations of at least 40 years were included in our analysis. The median absolute deviation (MAD) method[41,42] was then used to identify and exclude potentially erroneous records of LUD. For each species at each site, the MAD was calculated as: MAD = median ($|LUD_i$ – median (LUD_1, LUD_2, … LUD_n)|), where $LUD_{1,\,i,\,n}$ are the

LUD in the 1^{th}, i^{th} and n^{th} observation year, respectively. Any record deviating by more than 3 times the MAD was considered as an outlier and removed from the original dataset used in this study. After MAD pre-treatment, > 300,000 LUD records were left for further analysis.

Daily mean elevation and air temperature at each site were obtained from the gridded database E-OBS (http://ensembles-eu.metoffice.com) at a spatial resolution of 0.1° (approximately 10 km)[43]. Due to the relatively coarse spatial resolution of the E-OBS database, the elevation of some phenological sites may be vastly different from the mean elevation of the grid cells where they locate, especially in mountainous areas. To reach a more accurate quantification of temperature at each site, the temperature data from E-OBS were adjusted using the difference between the actual elevation at each site (as specified in the PEP database) and the mean elevation of the corresponding grid cell (as specified in E-OBS). The temperature lapse rate is set to 0.64 °C per 100 m change in elevation[44].

The Unified phenology model Phenological models are generally developed based on distinct assumptions regarding the response of bud growth to spring thermal accumulation and/or winter chilling[34,35]. For example, the Thermal Time model considers that only forcing temperatures explain the LUD[22]. More sophisticated models also consider the effect of chilling temperatures on bud dormancy breaking. For example, the Sequential model assumes that the effect of forcing temperatures cannot be effective unless chilling requirements have already been fulfilled[45]. In contrast, the Parallel model assumes that forcing temperatures can be active concomitantly with chilling accumulation[45]. Furthermore, in other models such as the Alternating model, the thermal accumulation required for leaf unfolding is assumed to decline exponentially with increasing chilling accumulation[20]. These models are non-

329 nested within each other and , therefore, cannot be used to test the effects of the above
330 assumptions on the response of LUD to chilling and forcing temperatures
331 simultaneously[19]. To circumvent these limitations, we applied the Unified phenology
332 model[19] in our study.

333 The Unified phenology model[19] allows for a direct estimation of the response of
334 spring phenology to both chilling and forcing temperatures, and of the periods when
335 these temperatures affect the plant phenology. In addition, it integrates the main
336 assumptions of simpler phenology models, in particular the sequential[45], parallel[34] and
337 alternating[20] models, which can in fact be regarded as particular cases of the Unified
338 model. Moreover, previous studies have indicated that the Unified model generally
339 provides more accurate estimations of the LUD of European trees than other
340 commonly used models[7].

341 In the Unified model, the daily chilling rate (CH_r, unitless) during cold days is
342 calculated using a unimodal function (Fig. S2a) of daily mean air temperature (T, °C):

343 $$CH_r = \frac{1}{e^{c_1(T-T_{op})^2+c_2(T-T_{op})}} \quad (1)$$

344 where T_{op} is the optimal chilling temperature, and c_1 and c_2 are two calibration
345 coefficients (Table S2). With specific values of T_{op}, c_1 and c_2, Eq.1 can capture other
346 widely used chilling metrics[19] such as, the chilling days (CH_r = 1 if T⩽5 °C; CH_r = 0
347 if T⩽5 °C) (Figs. S10a,b). Bud dormancy is released (d_{f0}) when the accumulation of
348 daily chilling rate since a specific day (d_{c0}, the start day of chilling accumulation)
349 exceeds the plants' critical chilling requirement (CHA_0, unitless), i.e. when
350 $\sum_{d_{c0}}^{d_{f0}} CH_r > CHA_0$. Note that d_{f0} also corresponds to the start day of forcing (thermal)

accumulation (Fig. S2). The daily forcing rate (F_r, unitless) is calculated using a sigmoid function (Fig. S2a) of daily mean air temperature (T, °C):

$$F_r = \frac{1}{1.0+e^{c_3(T-T_{50})}} \quad (2)$$

where T_{50} is the mid-response temperature, which induces 50% of optimal growth in forcing rate and is the inflection point of the function. c_3 is a calibration coefficient. Leaf unfolding occurs when the forcing accumulation ($\sum_{d_{f0}}^{LUD} F_r$) exceeds a certain thermal requirement (TA_0) which declines exponentially with the total chilling accumulation (CHA_{tot}) during the whole pre-growing season (i.e. period from the start day of chilling accumulation to the LUD) (Fig. S2b in SI):

$$TA_0 = c_4\, e^{c_5\, CHA_{tot}} \quad (3)$$

$$CHA_{tot} = \sum_{d_{c0}}^{LUD} CH_r \quad (4)$$

where c_4 and c_5 are two calibration coefficients. The important point to understand in this model is that after dormancy break, chilling temperature continue to have an effect on CHA_{tot} and forcing requirement decreases as CHA_{tot} increases.

Parameter estimation and model application Nine parameters of the Unified model, including the start day of chilling accumulation (d_{c0}), the critical chilling requirement for releasing bud dormancy (CHA_0), the optimal chilling temperature (T_{op}), the mid-response temperature (T_{50} in Eq. 2) and the five coefficients c_1 to c_5 in Eqs. 1-3, were optimized for each species at each site using an effective global optimization algorithm-the shuffled complex evolution algorithm (SEC-UA)[46]. Prior value and the range of each parameter to be optimized are listed in Table S2. Root mean square error (RMSE, Eq. 5) between simulated (LUD_{sim_i}) and observed

374 (LUD_{obs_i}) LUDs was used as the objective function, and parameter valuess that
375 minimized the RMSE were regarded as optimal.

376 $$RMSE = \sqrt{\left(\frac{\sum_{i=1}^{n}(LUD_{sim\_i} - LUD_{obs\_i})^2}{n}\right)} \quad (5)$$

377 where n is the number of LUD records (years) for each species at each site.

378 Using the optimized parameters, the Unified model was then applied to estimate the
379 day of bud dormancy release, total winter chilling accumulation, daily forcing rate
380 and the LUD for each year, each species and each site. We divided the whole 1951-
381 2019 period into three shorten timespans: 1951-1979, 1980-1999 and 2000-2019.
382 Analysis of the time series of LUD, mean winter temperature and mean spring
383 temperature showed that the LUD and temperature were overall stable in Europe
384 during 1951-1979 (Figs. S15 and S16). During the 1980-1999 period, the spring
385 temperature in Europe increased significantly and the LUD advanced quickly, by up
386 to 0.5 day yr^{-1}. During 2000-2019, the spring temperature in Europe was again overall
387 stable, while winter temperature increased significantly (Figs. S15 and S16). For each
388 of these three timespan, in addition to the average value of LUD, spring and winter
389 temperatures, we also calculated the metrics needed to constrain winter chilling and
390 spring forcing. The changes in each variable was then computed and their significance
391 was evaluated using an independent t-test.

392 In the Unified model, the LUD is determined by the time when bud dormancy is
393 released (which itself depends on the daily rate of chilling accumulation), the rate of
394 forcing accumulation and the required amount of forcing (TA_0) required for leaf
395 unfolding (Fig. S2). To assess the relative contributions of these three factors to the
396 temporal shifts in LUD, we expressed their effects in number of days. We first
397 calculated the changes in the date of bud dormancy break (d_{f0} in Fig. S2c) from the

period 1951-1979 (d_{f0_1970s}) to periods 1980-1999 (d_{f0_1990s}) and 2000-2019 (d_{f0_2010s}) (Eqs. 6 & 7) for each tree species at each site (ΔD_{df0}, Figs. 2 & S4).

$$\Delta D_{df0\_1990s} = d_{f0\_1990s} - d_{f0\_1970s} \quad (6)$$

$$\Delta D_{df0\_2010s} = d_{f0\_2010s} - d_{f0\_1970s} \quad (7)$$

Second, to estimate the shifts in LUD caused by the increased thermal accumulation (ΔD_{TA0} in Fig. 1) required for leaf unfolding due to warming-induced loss of winter chilling, we simulated the LUD for each species at each site for the two more recent timespans (1981-2019) by fixing the TA_0 in the Unified model to the average TA_0 corresponding to the 1951-1979 period. From the period 1951-1979 to periods 1980-1999 and 2000-2019, the ΔD_{TA0} was then calculated as the difference between the simulated LUDs using the 1951-1979 TA_0 (LUD_{TA0_1970s}) and the LUDs calculated on the basis of the actual total winter chilling accumulation for each year using Eq. 3 (LUD_{TA0_1990s} and LUD_{TA0_2010s}) (Eqs. 8 & 9).

$$\Delta D_{TA0\_1990s} = LUD_{TA0\_1990s} - LUD_{TA0\_1970s} \quad (8)$$

$$\Delta D_{TA0\_2010s} = LUD_{TA0\_2010s} - LUD_{TA0\_1970s} \quad (9)$$

Third, the contribution of warming-induced changes in daily forcing rates to shifts in LUDs (ΔD_{FD}) was calculated as the changes in the duration of the forcing stage (FD, i.e. the number of days from d_{f0} to LUD) from the period 1951-1979 (FD_{1970s}) to the periods 1980-1999 (FD_{1990s}) and 2000-2019 (FD_{2010s}) respectively, but excluding the influence of TA0 changes on this temporal shift:

$$\Delta D_{FD\_1990s} = FD_{1990s} - FD_{1970s} - \Delta D_{TA0\_1990s} \quad (10)$$

$$\Delta D_{FD\_2010s} = FD_{2010s} - FD_{1970s} - \Delta D_{TA0\_2010s} \quad (11)$$

Finally, the relative contributions of ΔD_{df0} ($p\Delta D_{df0}$), ΔD_{FD} ($p\Delta D_{FD}$) and ΔD_{TA0} ($p\Delta D_{TA0}$) to the shifts in LUD were calculated as follows:

$$p\Delta D_{df0} = \left(\frac{|\Delta D_{df0}|}{|\Delta D_{df0}|+|\Delta D_{FD}|+|\Delta D_{TA0}|}\right) \times 100\% \quad (12)$$

$$p\Delta D_{FD} = \left(\frac{|\Delta D_{FD}|}{|\Delta D_{df0}|+|\Delta D_{FD}|+|\Delta D_{TA0}|}\right) \times 100\% \quad (13)$$

$$p\Delta D_{TA0} = \left(\frac{|\Delta D_{TA0}|}{|\Delta D_{df0}|+|\Delta D_{FD}|+|\Delta D_{TA0}|}\right) \times 100\% \quad (14)$$

Temperature sensitivity of LUD The temperature sensitivity of LUD (S_T, day °C^{-1}) was first calculated for each species at each site based on a linear least square regression analysis of LUD and mean preseason temperature, defined as the period from the start date of chilling accumulation (d_{c0} in Fig. 3) to the mean LUD. The slope of the linear regression line was then used to quantify S_T. In addition, we also calculated the S_T when the preseason for each species at each site is defined as the period (with 5-day steps) for which the absolute value of the correlation coefficient between LUD and air temperature was highest during 1951-2019, i.e. the period which is most relevant to leaf unfolding[7]. In this case, we first calculated the mean temperature during each of the 27 periods ranging from 20 to 150 days (i.e. 20, 25, … , 145, 150, each at 5 day intervals) preceding the mean LUD. Pearson's correlation coefficients were calculated between the LUD and the mean temperature during each of these 27 periods. The period during which the absolute value of correlation coefficient between LUD and mean air temperature was highest was regarded as the optimal preseason.

To estimate the trend in the temporal change of the temperature sensitivity of LUD, we also conducted a reduced major axis regression for each species at each site with a

15-year moving window from 1951 to 2019, that is, we calculated the temperature sensitivity for each continuous 15 years over the entire record period.

Data and code availability

Phenology data are available from the Pan European Phenology (PEP) network (http://www.pep725.eu). Climate data can be downloaded from E-OBS site: http://ensembles-eu.metoffice.com. The codes of the Unified model and the program (SCE-UA algorithm) used for parameterization can be found in the supplementary materials. All programs for data analysis used in this study can be obtained by contacting the corresponding author.

Acknowledgements

HZ and PR acknowledges the 'Lateral-CNP' project (No. 34823748) supported by the Fonds de la Recherche Scientifique –FNRS and the VERIFY project funded by the European Union's Horizon 2020 research and innovation program under grant agreement No. 776810. We acknowledge all members of the PEP725 network for collecting and providing the phenological data.

Author contributions

Competing interests

The authors declare no competing interests.

464

References

1 Arora, V. K. & Boer, G. J. A parameterization of leaf phenology for the terrestrial ecosystem component of climate models. *Global Change Biology* **11**, 39-59, doi:10.1111/j.1365-2486.2004.00890.x (2005).

2 Richardson, A. D. *et al.* Terrestrial biosphere models need better representation of vegetation phenology: results from the North American Carbon Program Site Synthesis. *Global Change Biology* **18**, 566-584, doi:10.1111/j.1365-2486.2011.02562.x (2012).

3 Peñuelas, J., Rutishauser, T. & Filella, I. Ecology. Phenology feedbacks on climate change. *Science* **324**, 887-888, doi:10.1126/science.1173004 (2009).

4 Richardson, A. D. *et al.* Influence of spring and autumn phenological transitions on forest ecosystem productivity. *Philos Trans R Soc Lond B Biol Sci* **365**, 3227-3246, doi:10.1098/rstb.2010.0102 (2010).

5 Diez, J. M. *et al.* Forecasting phenology: from species variability to community patterns. *Ecol Lett* **15**, 545-553, doi:10.1111/j.1461-0248.2012.01765.x (2012).

6 Hegland, S. J., Nielsen, A., Lazaro, A., Bjerknes, A. L. & Totland, O. How does climate warming affect plant-pollinator interactions? *Ecol Lett* **12**, 184-195, doi:10.1111/j.1461-0248.2008.01269.x (2009).

7 Fu, Y. H. *et al.* Declining global warming effects on the phenology of spring leaf unfolding. *Nature* **526**, 104-107, doi:10.1038/nature15402 (2015).

8 Zhang, H., Yuan, W., Liu, S. & Dong, W. Divergent responses of leaf phenology to changing temperature among plant species and geographical regions. *Ecosphere* **6**, art250, doi:10.1890/es15-00223.1 (2015).

9 Zhang, G., Zhang, Y., Dong, J. & Xiao, X. Green-up dates in the Tibetan Plateau have continuously advanced from 1982 to 2011. *Proc Natl Acad Sci U S A* **110**, 4309-4314, doi:10.1073/pnas.1210423110 (2013).

10 Menzel, A. *et al.* European phenological response to climate change matches the warming pattern. *Global Change Biology* **12**, 1969-1976, doi:10.1111/j.1365-2486.2006.01193.x (2006).

11 Cleland, E. E., Chuine, I., Menzel, A., Mooney, H. A. & Schwartz, M. D. Shifting plant phenology in response to global change. *Trends Ecol Evol* **22**, 357-365, doi:10.1016/j.tree.2007.04.003 (2007).

12 Menzel, A., Sparks, T. H., Estrella, N. & Roy, D. B. Altered geographic and temporal variability in phenology in response to climate change. *Global Ecology and Biogeography* **15**, 498-504, doi:10.1111/j.1466-822X.2006.00247.x (2006).

13 Zhang, X., Tarpley, D. & Sullivan, J. T. Diverse responses of vegetation phenology to a warming climate. *Geophysical Research Letters* **34**, doi:10.1029/2007gl031447 (2007).

14 Fitter, A. H. & Fitter, R. S. Rapid changes in flowering time in British plants. *Science* **296**, 1689-1691, doi:10.1126/science.1071617 (2002).

15 Primack, R. B. *et al.* Spatial and interspecific variability in phenological responses to warming temperatures. *Biological Conservation* **142**, 2569-2577, doi:10.1016/j.biocon.2009.06.003 (2009).

16 Cleland, E. E., Chiariello, N. R., Loarie, S. R., Mooney, H. A. & Field, C. B. Diverse responses of phenology to global changes in a grassland ecosystem. *Proc Natl Acad Sci U S A* **103**, 13740-13744, doi:10.1073/pnas.0600815103 (2006).

17 Wang, H., Dai, J., Zheng, J. & Ge, Q. Temperature sensitivity of plant phenology in temperate and subtropical regions of China from 1850 to 2009. *International Journal of Climatology* **35**, 913-922, doi:10.1002/joc.4026 (2015).

18 Chuine, I. M., Xavier; Bugmann, Harald. Warming, Photoperiods, and Tree Phenology. *Science* **329**, 277-278 (2010).
19 Chuine, I. A unified model for budburst of trees. *J Theor Biol* **207**, 337-347, doi:10.1006/jtbi.2000.2178 (2000).
20 Murray, M., Cannell, M. G. R. & Smith, R. I. Date of budburst of fifteen tree species in Britain following climatic warming. *Journal of Applied Ecology* **26**, 693-700, doi:DOI:10.2307/2404093 (1989).
21 Man, R., Lu, P. & Dang, Q. L. Insufficient Chilling Effects Vary among Boreal Tree Species and Chilling Duration. *Front Plant Sci* **8**, 1354, doi:10.3389/fpls.2017.01354 (2017).
22 Cannell, M. G. R. & Smith, R. I. L. Thermal time, chill days and prediction of budburst in Picea sitchensis. *J. Appl. Ecol.* **20**, 951-963 (1983).
23 Fu, Y. H. *et al.* Increased heat requirement for leaf flushing in temperate woody species over 1980-2012: effects of chilling, precipitation and insolation. *Glob Chang Biol* **21**, 2687-2697, doi:10.1111/gcb.12863 (2015).
24 Zhang, H., Liu, S., Regnier, P. & Yuan, W. New insights on plant phenological response to temperature revealed from long-term widespread observations in China. *Glob Chang Biol* **24**, 2066-2078, doi:10.1111/gcb.14002 (2018).
25 Yu, H., Luedeling, E. & Xu, J. Winter and spring warming result in delayed spring phenology on the Tibetan Plateau. *Proc Natl Acad Sci U S A* **107**, 22151-22156, doi:10.1073/pnas.1012490107 (2010).
26 Asse, D. *et al.* Warmer winters reduce the advance of tree spring phenology induced by warmer springs in the Alps. *Agricultural and Forest Meteorology* **252**, 220-230, doi:10.1016/j.agrformet.2018.01.030 (2018).
27 Ettinger, A. K. *et al.* Winter temperatures predominate in spring phenological responses to warming. *Nature Climate Change* **10**, 1137-1142, doi:10.1038/s41558-020-00917-3 (2020).
28 Chuine, I. & Régnière, J. Process-Based Models of Phenology for Plants and Animals. *Annual Review of Ecology, Evolution, and Systematics* **48**, 159-182, doi:10.1146/annurev-ecolsys-110316-022706 (2017).
29 Caffarra, A., Donnelly, A., Chuine, I. & Jones, M. B. Modelling the timing of Betula pubescens budburst. I. Temperature and photoperiod: a conceptual model. *Climate Research* **46**, 147-157, doi:10.3354/cr00980 (2011).
30 Luterbacher, J., Dietrich, D., Xoplaki, E., Grosjean, M. & Wanner, H. European Seasonal and Annual Temperature Variability, Trends, and Extremes Since 1500. *Science* **303**, 1499-1503, doi:10.1126/science.1093877 (2004).
31 Ciais, P. *et al.* in *Climate Change 2013: The Physical Science Basis. Contribution of Working Group I to the Fifth Assessment Report of the Intergovernmental Panel on Climate Change* (eds T.F. Stocker *et al.*) (Cambridge University Press, Cambridge, United Kingdom and New York, NY, USA, 2013).
32 Fu, Y. H. *et al.* Daylength helps temperate deciduous trees to leaf-out at the optimal time. *Glob Chang Biol* **25**, 2410-2418, doi:10.1111/gcb.14633 (2019).
33 Templ, B. *et al.* Pan European Phenological database (PEP725): a single point of access for European data. *Int J Biometeorol* **62**, 1109-1113, doi:10.1007/s00484-018-1512-8 (2018).
34 Kramer, K. Selecting a model to predict the onset of growth of Fagus sylvatica. *Journal of Applied Ecology* **31**, 172-181, doi:10.2307/2404609 (1994).
35 Chuine, I., Cour, P. & Rousseau, D.-D. Selecting models to predict the timing of flowering of temperate trees: implications for tree phenology modelling. *Plant Cell and Environment* **22**, 1-13 (1999).

564 36 Zhang, H., Yuan, W., Liu, S., Dong, W. & Fu, Y. Sensitivity of flowering phenology to
565 changing temperature in China. *Journal of Geophysical Research: Biogeosciences*
566 **120**, 1658-1665, doi:10.1002/2015jg003112 (2015).
567 37 Richardson, A. D. *et al.* Influence of spring phenology on seasonal and annual carbon
568 balance in two contrasting New England forests. *Tree Physiol* **29**, 321-331,
569 doi:10.1093/treephys/tpn040 (2009).
570 38 Körner, C. & Basler, D. Phenology Under Global Warming. *Science* **327**, 1461-1462,
571 doi:10.1126/science.1186473 (2010).
572 39 Zohner, C. M. & Renner, S. S. Common garden comparison of the leaf-out phenology
573 of woody species from different native climates, combined with herbarium records,
574 forecasts long-term change. *Ecol Lett* **17**, 1016-1025, doi:10.1111/ele.12308 (2014).
575 40 Vitasse, Y. & Basler, D. What role for photoperiod in the bud burst phenology of
576 European beech. *European Journal of Forest Research* **132**, 1-8, doi:10.1007/s10342-
577 012-0661-2 (2012).
578 41 Chen, L. *et al.* Leaf senescence exhibits stronger climatic responses during warm
579 than during cold autumns. *Nature Climate Change* **10**, 777-780, doi:10.1038/s41558-
580 020-0820-2 (2020).
581 42 Leys, C., Ley, C., Klein, O., Bernard, P. & Licata, L. Detecting outliers: Do not use
582 standard deviation around the mean, use absolute deviation around the median.
583 *Journal of Experimental Social Psychology* **49**, 764-766,
584 doi:10.1016/j.jesp.2013.03.013 (2013).
585 43 Beer, C. *et al.* Harmonized European Long-Term Climate Data for Assessing the Effect
586 of Changing Temporal Variability on Land–Atmosphere CO2 Fluxes. *Journal of*
587 *Climate* **27**, 4815-4834, doi:10.1175/jcli-d-13-00543.1 (2014).
588 44 Olsson, C. & Jönsson, A. M. Process-based models not always better than empirical
589 models for simulating budburst of Norway spruce and birch in Europe. *Global*
590 *change biology* **20 11**, 3492-3507 (2014).
591 45 Hänninen, H. Modelling bud dormancy release in trees from cool and temperate
592 regions. *Acta For. Fenn.* **14**, 499-454 (1990).
593 46 Duan, Q., Sorooshian, S. & Gupta, V. K. Optimal use of the SCE-UA global
594 optimization method for calibrating watershed models. *Journal of Hydrology* **158**,
595 265-284, doi:10.1016/0022-1694(94)90057-4 (1994).

596•

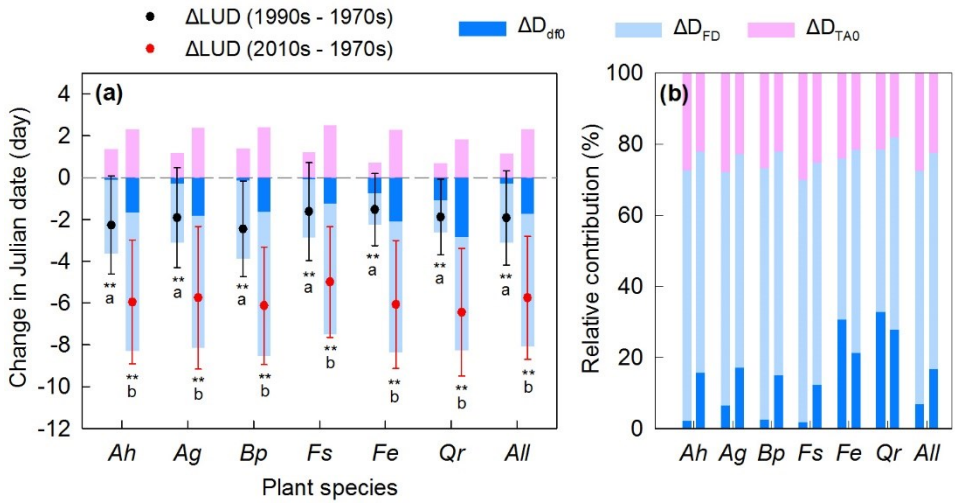

Figure 1 | Changes in the leaf unfolding days (ΔLUD) of six plant species in Europe from 1951 to 2019 and the potential absolute (a) and relative (b) contributions of changes in winter chilling and spring forcing to the ΔLUD. The negative value denotes an advance of LUD; otherwise, the negative value denotes a delayed LUD. The black and red dots show the average ΔLUD between 1980-1999 (black), 2000-2019 (red) and 1951-1979, respectively. Error bars denote the standard deviation of ΔLUD at different observation sites. The asterisks (**) indicate the changes in LUD are significantly different from zero (p<0.01), and the different letters (a, b) below asterisks means the average LUDs in 1980-1999 are significantly different from that in 2000-2019 (p<0.01). ΔD_{df0} is the changes in date when dormancy is released. ΔD_{FD} is the potential changes in the duration (day) of forcing stage caused by changes in spring forcing temperatures. ΔD_{TA0} is the potential shifts in LUD caused by changes in plants' critical requirement of thermal accumulation. *AH* denotes *Aesculus hippocastanum*; *AG* denotes *Alnus glutinosa*; *BP* is *Betula pendula*; *FS* is *Fagus sylvatica*; *FE* is *Fraxinus excelsior*; *QR* is *Quercus robur*; *All* represents the average values for all of the six species.

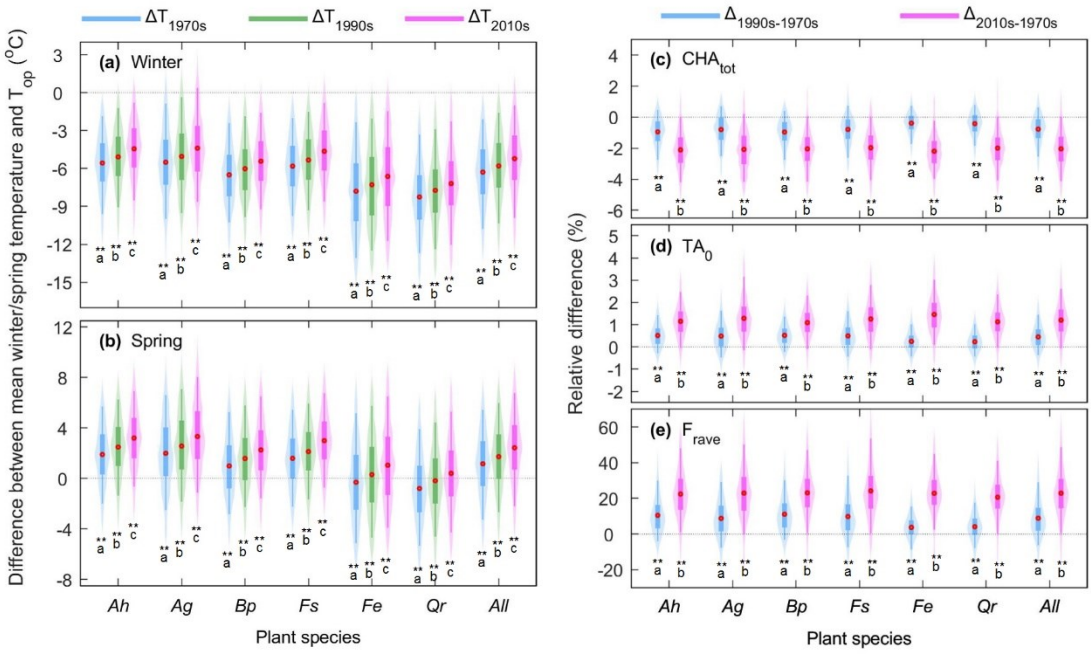

Figure 2 | Differences between mean winter (December-February) (a), mean spring (March-May) (b) temperatures and the optimal chilling temperature (T_{op}, °C) in 1951-1979 (ΔT_{1970s}), 1980-1999 (ΔT_{1990s}) and 2000-2019 (ΔT_{2010s}), and the relative changes in total chilling accumulation (CHA_{tot}) (c), the critical forcing accumulation required for leaf unfolding (TA_0) (d) and the average daily forcing rate during forcing stage (F_{rave}) (e) from 1951-1979 to 1980-1999 ($\Delta D_{1990s-1970s}$) and to 2000-2019 ($\Delta D_{1990s-1970s}$), respectively. In each violin plot, red dot is the mean value and balloon representing the probability density distribution of each value. Whiskers indicate the interquartile (thick) and 95 % confidence intervals (thin). The asterisks (**) indicate that the differences between winter/spring temperatures and T_{op} (a,b) or the relative changes in CHA_{tot} (c) or TA_0 (d) are significantly different from 0 ($p < 0.01$). For each plant species, the violins marked with different letters (i.e. a, b and c below the asterisks) are significantly different ($p<0.01$). *AH* denotes *Aesculus hippocastanum*; *AG* denotes *Alnus glutinosa*; *BP* is *Betula pendula*; *FS* is *Fagus sylvatica*; *FE* is *Fraxinus excelsior*; *QR* is *Quercus robur*; *All* denotes the average values for all of the six species.

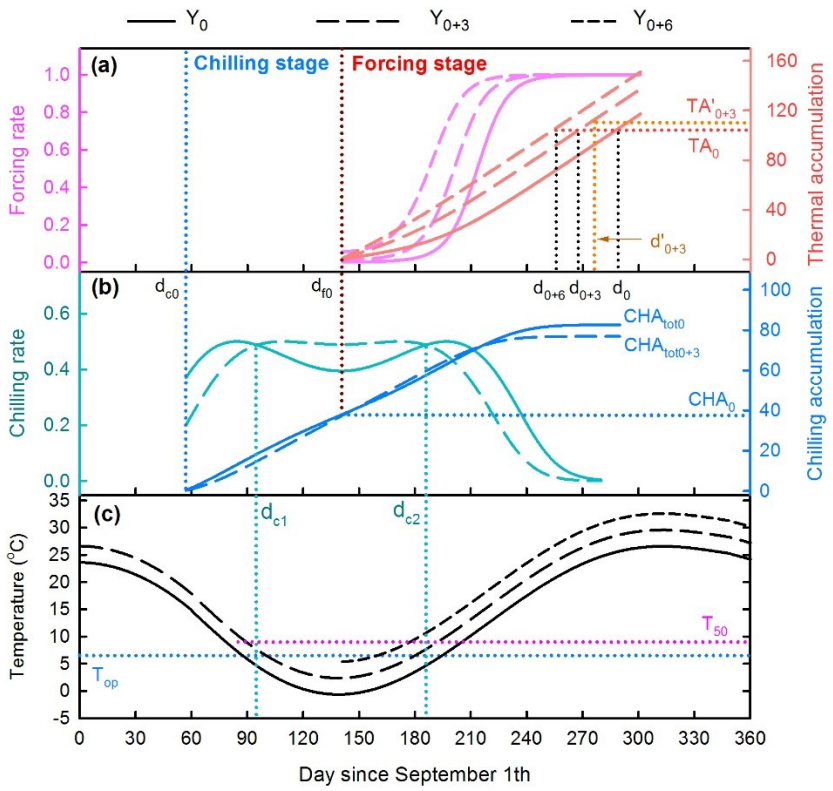

633

634 **Figure 3 | Schematic plot showing the impacts of rising temperatures (+3 and**
635 **+6 °C) on winter chilling, spring forcing and leaf unfolding day.** T_{op} is the optimal
636 chilling temperature (°C). CHA_0 is the critical chilling requirement for releasing
637 dormancy. CHA_{tot0} and CHA_{tot+3} are the total chilling accumulation in the reference
638 year (Y_0) and the year with 3 °C warming (Y_{0+3}), and TA_0 and TA_{+3} are the
639 corresponding critical forcing requirements for leaf. d_{c0} and d_{f0} are the start dates of
640 chilling and forcing accumulation, respectively in the reference year (Y_0). d_0, d_{0+3} and
641 d_{0+6} are the leaf unfolding dates in the reference year Y_0 and the years with +3°C and
642 +6°C warming if the chilling accumulation would have been identical to the reference
643 year (CHA_{tot0}). d'_{0+3} is the leaf unfolding date in Y_{0+3} when considering the lower
644 chilling accumulation (CHA_{tot+3}) induced by warming and responsible for a higher
645 forcing requirements. d_{c1} and d_{c2} represents the start and end dates of the period when
646 temperature in Y_{0+3} is more efficient for chilling accumulation (because closer to T_{op})
647 than the temperature in Y_0.
648

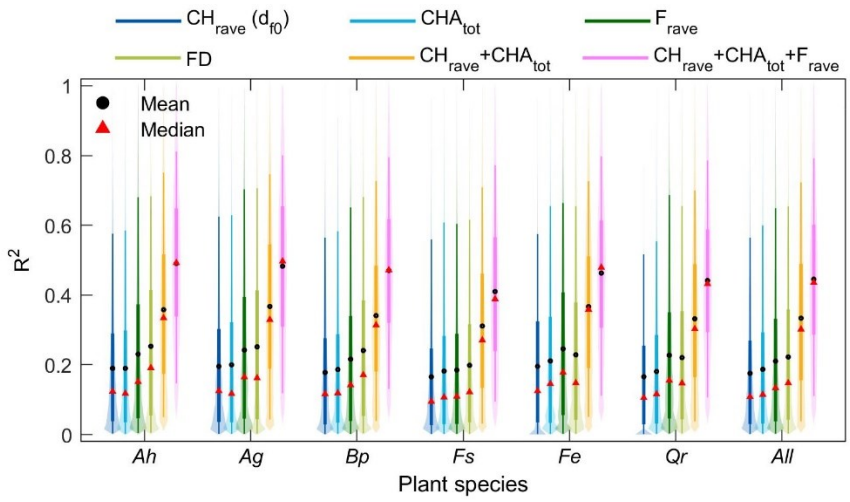

649

650 **Figure 4 | Determining coefficients (R^2) of the linear regression function between**
651 **the temperature sensitivity of LUD and different metrics of winter chilling and**
652 **spring forcing.** CH_{rave} is the average daily chilling rate from the start date of chilling
653 accumulation (i.e. d_{c0} in Fig. 3) to the start date of forcing accumulation (d_{f0}). CHA_{tot}
654 is the total chilling accumulation in the whole pre-growing season. F_{rave} is the average
655 daily forcing rate during the forcing stage. DF is the duration of forcing stage (day).
656 CH_{rave} +CHA_{tot} refers to the regression using both CH_{rave} and CHA_{tot} as independent
657 variables, and CH_{rave} +CHA_{tot} +F_{rave} refers to the regression using CH_{rave}, CHA_{tot} and
658 F_{rave} together as independent variables. In each violin plot, balloon represents the
659 probability density distribution of each gradient of R^2. Whiskers indicate the
660 interquartile (thick) and 95 % confidence intervals (thin). *AH* denotes *Aesculus*
661 *hippocastanum*; *AG* denotes *Alnus glutinosa*; *BP* is *Betula pendula*; *FS* is *Fagus*
662 *sylvatica*; *FE* is *Fraxinus excelsior*; *QR* is *Quercus robur*; *All* denotes the average
663 values for all of the six species.
664

Supplementary Files

This is a list of supplementary files associated with this preprint. Click to download.

- SupplementaryInformation.pdf